

Membranes obtained on the basis of cellulose acetate and their use in removal of phenol from liquid phase

Joanna Przybyl¹, Aleksandra Bazan-Wozniak¹, Agnieszka Nosal-Wiercinska², Robert Pietrzak^{1*}

¹ Adam Mickiewicz University in Poznań, Faculty of Chemistry, Uniwersytetu Poznańskiego 8, 61-614 Poznań, Poland

² Maria Curie-Skłodowska University in Lublin, Faculty of Chemistry, Department of Analytical Chemistry, Institute of Chemical Sciences, Maria Curie-Skłodowska 3, 20-031 Lublin, Poland

Corresponding author: pietrob@amu.edu.pl (Robert Pietrzak)

Abstract: The membranes based on cellulose acetate (CA) were obtained by the method of phase inversion and used for removal of phenol (in concentrations of 15 and 25 mg/L) from liquid phase. To differentiate the hydrophilic properties of the membrane surfaces, different amounts of cellulose acetate (14 and 18 wt. %) and polyvinylpyrrolidone as a pore-generating agent (PVP, 1, 2, 3 or 4 wt. %) were used. The membranes were characterised by determination of their porosity, equilibrium water content, wetting angle and content of surface oxygen functional groups. After the application of membranes to phenol removal, the following parameters characterising the process were determined: permeability, membrane resistance, cake resistances, pore resistances, total filtration resistance and flux recovery ratio. The membranes were found to show higher effectiveness in phenol removal from a solution of the initial concentration 15 mg/L, and more effective were the membranes with higher contents of cellulose acetate. On the surface of the membranes the oxygen functional groups of acidic nature are dominant, both before and after filtration. The membranes of higher contents of cellulose acetate show higher resistances.

Keywords: cellulose acetate membrane, phase inversion, physical and chemical properties, surface chemistry, phenol removal

1. Introduction

Increasing degradation of the natural environment as a consequence of fast economic and industrial development forces not only improvement in the already introduced purification methods but also the search for new methods that would effectively remove pollutants from gas and liquid phases (Arasi et al., 2021; Bazan and Pietrzak, 2020; Gnanasekaran et al., 2021). Important effective methods applied for purification are those based on the membrane separation (Ding et al., 2020). The use of membranes based on organic polymers, permits the removal of organic and inorganic chemical compounds (Leon et al., 2016; Pan et al., 2019). The membranes used for purification of water solutions can have the forms of capillary tubes, hollow fibres or plane sheets (Hou et al., 2014; HoogAntink et al., 2019). The most popular method for the production of membranes is the phase inversion, which permits obtaining membranes from such polymers as polyvinylidene fluoride, cellulose acetate, polysulphone or polyethersulphone (Kamal et al., 2020; Thomas et al., 2014; Ocakoglu et al., 2021). In this method, a mixture of the polymer, solvent and pore-generating agent is smeared out on a solid substrate, e.g. on the glass, with a knife, the solvent is evaporated and then the substrate with the layer of polymer and pore-generating agent is immersed in the coagulating bath, e.g. with deionised water (Krason and Pietrzak, 2018). As a result, asymmetric porous membranes in the form of plane sheets are obtained.

One of the frequently met pollutants is phenol, which is the compound used in many branches of industry and thus it is discharged with waste waters from many plants (Paul et al., 2021). It is a toxic substance, when in contact with skin it causes irritation and after intake it causes headaches, problems with metabolism, damages to the heart, kidneys and liver (Rudzanova et al., 2019; Solomakaou and

Goula, 2021). Phenol is also damaging to water environment as it causes for example the oxidative stress in water organisms, so it is essential to prevent its penetration to surface and underground waters (Sari et al., 2020). The most popular methods for phenol removal are adsorption on e.g. zeolites, activated carbon or membranes as in this study (Bera et al., 2016; Hernandez-Barreto et al., 2020; Wu et al., 2021). The use of membranes is very attractive as it does not require complex technological processes (Fang et al., 2022).

The main aim of this study was to obtain membranes of different contents of pore-generating agent, based on cellulose acetate by the method of phase inversion and characterise their performance in the process of removal of phenol from liquid phase.

2. Materials and methods

2.1. Materials

Cellulose acetate (CA) was purchased from Sigma Aldrich and used as a membrane material. *N,N*-dimethylformamide (DMF) was purchased from Avantor Performance Materials Poland S.A. and used as a solvent. Polyvinylpyrrolidone (PVP, 10 000 g/mol) as a pore former was supplied by Sigma Aldrich.

2.2. Preparation of CA membranes

Casting solutions of CA 14 or 18 wt. % and 1, 2, 3 or 4 wt. % of PVP were prepared by mixing the ingredients in a flask. The casting solution obtained was left to rest for about 24 h to allow complete release of bubbles. After that, it was cast onto a glass plate using a stainless-steel knife to get a casting film of 300 μm thickness, exposed to the atmosphere for 40 s, and then immersed into a coagulation bath of deionized water. The as-prepared cast solution films were immersed and kept for 24 h in a deionised water bath conditioned at 25°C to complete the exchange between the solvent and non-solvent. Directly prior to use, each electrode was washed with a small amount of deionised water.

2.3. Membrane structure characterization

The membrane porosity was determined by the mass loss of wet membrane after drying. The membrane sample was mopped with water on the surface and weighed under wet status. Then, the membrane sample was dried in a drier at 60 °C for 24 h. The membrane porosity ε (%) (Jasiewicz and Pietrzak, 2013) was evaluated from equation:

$$\varepsilon = \frac{W_w - W_d}{\rho \cdot v} \cdot 100\% \quad (1)$$

where W_w is the mass of a wet membrane sample (g), W_d is the mass of dry state membrane sample (g), ρ - pure water density (g/cm^3) and v - is the volume of a membrane in wet state (cm^3).

The equilibrium water content (EWC) (Jasiewicz and Pietrzak, 2013) was determined by following formula:

$$EWC = \frac{W_w - W_d}{W_w} \cdot 100\% \quad (2)$$

The contact angle between water and membrane was directly measured using a contact angle measuring instrument G10, KRUSS, Germany. For evaluation of the membrane hydrophilicity deionized water was used as a probe liquid in all measurements. To minimize the experimental error, the contact angle was measured at five random locations for each sample and then the average was reported.

The surface properties were characterised using potentiometric titration experiments using 809 Titrand equipment manufactured by Metrohm. The instrument was set at the mode when the equilibrium pH was collected. Materials studied in the amount of about 0.05 g in 50 cm^3 0.01 mol/L NaNO_3 were placed in a container thermostated at 25°C and equilibrated overnight with the electrolyte solution. To eliminate the influence of atmospheric CO_2 , the suspension was continuously saturated with N_2 . The carbon suspension was stirred throughout the measurements. Volumetric standards NaOH (0.1 mol/L) or HCl (0.1 mol/L) were used as titrants (Hofman and Pietrzak, 2011; Szczepanik et al., 2019).

2.4. Membrane performance characterization

Water permeability of the membranes prepared was measured in a stainless steel cell, holding the effective membrane area of 19.6 cm². The membranes were initially subjected to deionised water of 3 bar for about 1.5 h before testing. Then, the pure water flux was measured at 3 bar, 23 ±1°C and 0.22 m/s cross-flow velocity. The pure water flux (Krason and Pietrzak, 2018) was calculated from the following equation:

$$J_w = \frac{V}{A \cdot \Delta t} \quad (3)$$

where J_w (L/(m²h)) is the pure water flux, V (L) is the volume of permeated water, A (m²) is the effective membrane area and Δt (h) is the permeation time.

The experiments were conducted using compressed nitrogen gas and phenol solutions of different initial concentrations (15 or 25 mg/L) and all measurements were made at 3 bar, in triplicate. The final concentration of phenol in the solution was analysed using a double beam UV-Vis spectrophotometer (Varian Cary 100 Bio) at 506 nm. The rejection of this compound (%R) (Zhao et al., 2013) were calculated from equation:

$$\%R = \left(1 - \frac{C_p}{C_f}\right) \cdot 100 \quad (4)$$

where C_p and C_f (mg/L) were phenol concentrations in the permeate and the feed solutions, respectively.

Membrane resistance was evaluated according to Darcy's law (Di Bella and Di Trapani, 2019) by the resistance in the series of models as follows:

$$J = \frac{\Delta P}{\mu R_t} \quad (5)$$

where J (L/(m²h)) is the permeate flux, ΔP is the transmembrane pressure (TMP) (Pa), μ is the dynamic viscosity of permeate (Pa·s), and R_t is the total filtration resistance (m/s). The resistance in the series of models combines various resistances causing flux decline as follows:

$$R_t = R_m + R_p + R_c \quad (6)$$

where, R_t is the total filtration resistance composed of various resistances including that of the membrane itself R_m , pore blocking R_p , cake resistance R_c . The intrinsic membrane resistance (R_m) can be estimated from the initial pure water flux. Fouling resistance (R_p) is caused by pore plugging and irreversible adsorption of foulants on membrane pore wall or surface. Cake resistance (R_c) induced by cake layer formed on the membrane surface was calculated from the water flux after pure water washing (Li et al., 2008; Basile and Gallucci, 2011)

The detail membrane fouling behaviour was studied as follows. Firstly, pure water flux of the membrane J_{w1} (L/(m²h)) was tested at 3 bar. Then, aqueous solution of phenol (15-25 mg/L) was fed into the ultrafiltration system. After filtration for 30 min, the membrane was flushed with pure water for 10 min and then pure water flux of the membrane J_{w2} (L/(m² h)) was measured. The flux recovery ratio (FRR) (Zhao et al., 2013) was calculated using the following formula:

$$FRR(\%) = \frac{J_{w2}}{J_{w1}} \cdot 100\% \quad (7)$$

3. Results and discussion

3.1. Membrane characterization

Table 1 presents the structural parameters and contact angles for the two series of membranes produced, CA14 and CA18.

Analysis of the results obtained for the membrane series CA14 shows that with increasing content of the pore-generating agent the total pore content at first decreases, when comparing the membranes with 1 and 2 % wt of PVP) and then increases. The values of equilibrium water content (EWC) show a similar tendency of changes, but they are very similar and change only from 82 to 83 %. The highest value of the contact angle was observed for the membrane of the lowest content of the pore-generating agent (CA14 PVP1), but the other membranes of 2, 3 and 4 % wt. of PVP showed stronger hydrophilic

properties, increasing with growing content of PVP. The decrease in the contact angle with increasing content of PVP can be related to the greater content of the polymer of hydrophilic surface.

Table 1. Porosity (ϵ), equilibrium water content (EWC) and contact angle of the membranes studied

Membrane	ϵ (%)	EWC (%)	Contact angle
CA14 PVP1	46.08	83.09	65.4±3.00
CA14 PVP2	43.23	82.50	52.6±7.68
CA14 PVP3	52.93	83.40	53.5±8.34
CA14 PVP4	52.93	83.70	54.4±2.98
CA18 PVP1	44.13	75.57	61.9±2.41
CA18 PVP2	50.31	76.74	62.8±1.47
CA18 PVP3	43.55	76.93	58.0±3.43

The porosity of CA18 series membranes did not depend on the content of PVP. The total pore content of the membranes containing 1, 3 and 4 % wt. of PVP changed from 43.55 to 44.54%. For sample CA18 PVP2 the total pore content is much greater and reaches 50.31 %. The EWC values are similar for all membranes and vary from 75 to 77 %. As follows from the contact angle measurements, it was higher for the membranes containing 1 and 2 % wt. PVP than for CA18 PVP3 and CA18 PVP4, so the former samples showed smaller hydrophilicity. The highest hydrophilicity was observed for the membrane with 3 % wt. PVP, while the lowest for that with 2 % wt. PVP.

3.2. Membrane performance

Tables 2 and 3 present the content of acidic and basic oxygen functional groups on the surfaces of the membranes, before and after the process of filtration of phenol solutions. The content of acidic oxygen functional groups on the surface of CA14 series samples increased only for sample CA14 PVP2, while on the surface of the other membranes from this series it decreased. For sample CA14 PVP2, the content of oxygen functional groups of basic character also increased, although this increase was much larger than that of acidic character. On the surfaces of the other membranes the contents of both acidic and basic oxygen functional groups decreased.

According to Table 2, the greatest decrease in their contents took place for sample CA14 PVP1. After the process of filtration, on the surface of sample CA14 PVP2 the content of oxygen functional groups increased, while on the surface of the other membranes from this series the content of oxygen functional groups decreased.

As follows from the data presented in Table 3, after the process of phenol solution filtration, on the surfaces of all membranes from series CA18 the content of oxygen functional groups of acidic character increased. Similarly, as for CA14 series membranes, the greatest increase in the content of oxygen functional groups of acidic character took place on sample CA14 PVP2, while on the surfaces of the other membranes this increase was not so significant. As far as the oxygen groups of basic character are concerned, after filtration the content of such groups on membranes CA18 PVP1 and CA18 PVP2 slightly increased, while on the surfaces of membranes CA18 PVP3 and CA18 PVP4 the content of such groups decreased, and this decrease was the greatest for the sample with the highest content of PVP. Analysis of the total number of surface oxygen functional groups showed that from among CA18 series

Table 2. Acidic and basic properties of CA14 series membranes before and after filtration of 25 mg/L phenol solution [mmol/g]

Sample	Acidic groups		Basic groups		Total content of oxygen groups	
	Before	After	Before	After	Before	After
CA14 PVP1	4.58	3.78	2.61	1.81	7.19	5.59
CA14 PVP2	4.51	4.71	1.72	3.67	6.23	8.38
CA14 PVP3	4.60	3.88	1.70	1.68	6.30	5.56
CA14 PVP4	4.42	4.30	1.65	1.61	6.07	5.91

Table 3. Acidic and basic properties of CA18 series membranes before and after filtration of 25 mg/L phenol solution [mmol/g]

Sample	Acidic groups		Basic groups		Total content of oxygen groups	
	Before	After	Before	After	Before	After
CA18 PVP1	4.37	4.58	1.52	1.68	5.89	6.26
CA18 PVP2	3.69	4.57	1.66	1.78	5.35	6.35
CA18 PVP3	4.00	4.14	1.63	1.54	5.63	5.68
CA18 PVP4	4.11	4.67	2.76	1.61	6.87	6.28

membranes, only for sample CA18 PVP4 this total number decreased. For the other membranes of this series an increase in the total number of oxygen functional groups was observed.

Fig. 1 presents the permeability determined before and after filtration of phenol solutions for CA14 series membranes. The permeability increased with increasing content of PVP from 1 to 3 % wt. from 55.36 L/m²h to 172.44 L/m²h. For membrane of the highest content of PVP, CA14 PVP4, the permeability decreased to 154.65 L/m²h. Irrespective of the content of PVP in the membranes, their permeabilities before filtrations were higher than after this process, which was a result of pore blocking. Usually, the permeabilities after filtrations were higher for the membranes used for the filtration of phenol solutions of the higher concentration of 25 mg/L, only for membrane CA14 PVP4 the permeability was higher after the filtration of phenol solution of the concentration 15 mg/L.

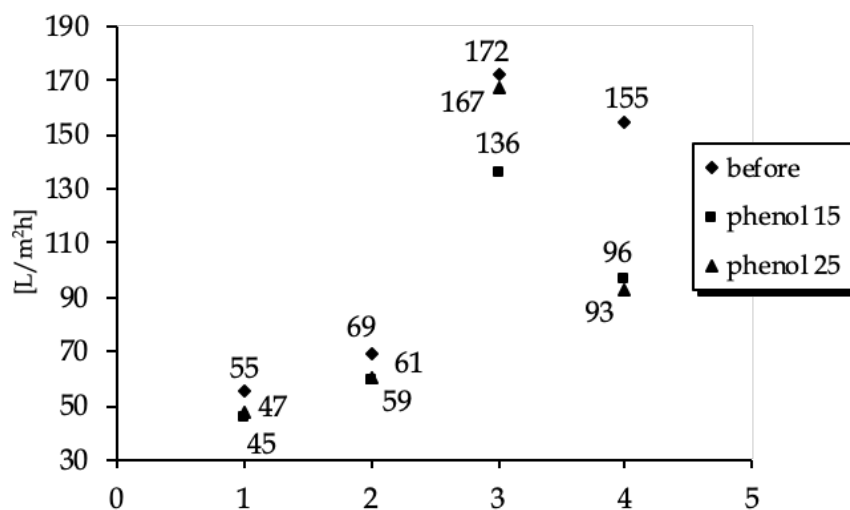


Fig. 1. Water flux of CA14 series membranes before and after phenol removal

Fig. 2 presents the permeability determined before and after the filtrations of phenol solutions for CA18 series membranes. For all membranes from this series, the permeabilities increase with increasing content of pore-generating agent. Before the filtrations the permeability of for membrane CA18 PVP1 was 7.15 L/m²h, while for the membrane of the highest content of PVP this value increased to 36.37 L/m²h. Similarly, as for membranes from CA14 series, the permeabilities before filtrations were higher than after this process. Analysis of the results obtained after the process of phenol solution filtrations shows that the permeabilities of membranes CA18 PVP1 and CA18 PVP4 are higher when the solution of the lower phenol concentration was used. For membranes CA18 PVP2 and CA18 PVP3, the flow rates are higher after the filtration of phenol solution of concentration 25 mg/L.

Fig. 3 presents the abilities of CA14 series membranes to remove phenol from water solutions. As follows from these data, the membranes from this series are more effective in removal of phenol from solutions of the concentration of 15 mg/L than from those of 25 mg/L. Irrespective of the phenol solution concentration, the volume of phenol removed from the liquid phase decreased with increasing content of PVP in the membranes. The exception was the fact that membrane CA14 PVP4 was more effective than CA14 PVP3 upon filtration of the solution of 25 mg/L.

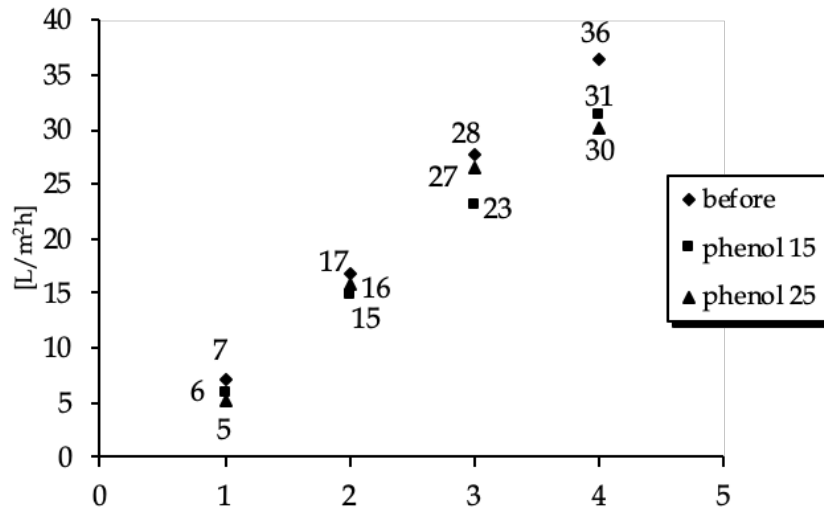


Fig. 2. Water flux of CA18 series membranes before and after phenol removal

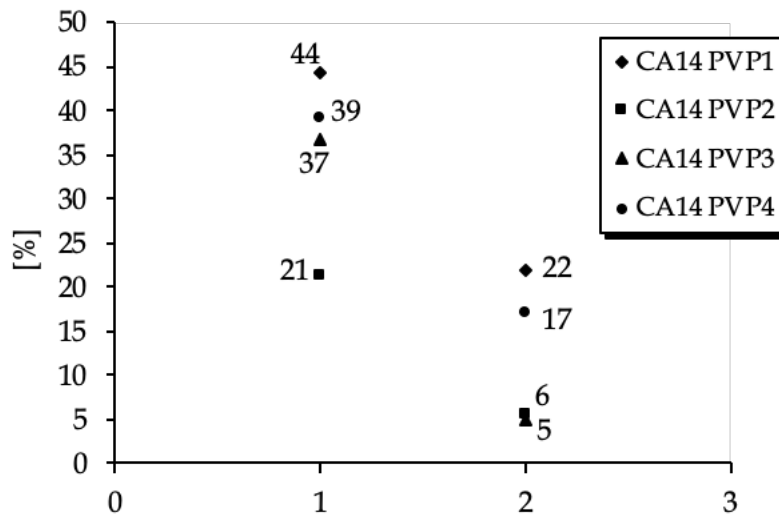


Fig. 3. Phenol rejection of CA14 series membranes after filtration of a phenol solution

The amount of phenol removed by membranes from series CA18 versus the content of PVP is illustrated in Fig. 4. The best performance was noted for membrane CA18 PVP2, which permitted the removal of 89.19 and 88.63 % of phenol from the solutions of concentrations 15 and 25 mg/L. Very effective in removal of phenol from the solution of concentration 15 mg/L was the membrane with the lowest content of PVP, but when the solution of phenol concentration 25 mg/L was used its effectiveness decreased. For membranes CA18 PVP3 and CA18 PVP4, the results were much poorer, they removed 41 and 46 % of phenol from the solution of concentration 15 mg/L and 21 and 28 % of phenol from the solution of 25 mg/L. Similarly, as for CA14 series membranes, the effectiveness of phenol removal depends on the initial concentration of the phenol solutions used for filtration.

Another parameter determined was the flux recovery ratio (FRR) after the filtrations of phenol solutions (Fig. 5). The FRR values for membranes CA14 PVP1 and CA18 PVP1 of the lowest content of PVP were 82 % and 73 %, respectively. For the membranes from series CA14 the FRR values increase with increasing content of PVP but only till membrane CA14 PVP3 for which the highest FRR of 96 % was observed. For membrane CA14 PVP4, the FRR value is much smaller and reached only 77 %. For the samples from series CA18 the values of FRR decreased from CA18 PVP2 with increasing content of PVP to reach 82 % for membrane CA18 PVP4.

The resistances determined for membranes from series CA14 after filtration of phenol solutions are displayed in Table 4.

The highest value of total resistance $R_t = 7.95 \times 10^{13}$ L/m²h was found for CA14 PVP1, so for the sample with the lowest content of PVP. The values for the other membranes were much lower and equalled to 5.05, 2.00 and 2.49 $\times 10^{13}$ L/m²h for the membranes of increasing content of PVP. For the values of the other particular resistances the tendencies are similar as for the total resistance. Table 5 presents the resistances determined after the filtration of phenol solutions for CA18 series membranes. The highest total resistance R_t of 54.20×10^{13} L/m²h was determined for membrane CA18 PVP1 and this value was much higher than those obtained for the other membranes. For the other ones the total resistance decreased with increasing content of PVP and took the values of 22.50, 11.52 and 10.04×10^{13} L/m²h. The values of particular components of the total resistance also showed clear dependence on the content of PVP.

Table 4. Filtration resistance of different membranes for phenol solution (25 mg/L)

Membrane	CA14 PVP1	CA14 PVP2	CA14 PVP3	CA14 PVP4
R_m ($\times 10^{13}$)	2.33	1.55	0.67	0.67
R_p ($\times 10^{13}$)	2.81	1.77	0.69	0.86
R_c ($\times 10^{13}$)	2.81	1.73	0.64	0.96
R_t ($\times 10^{13}$)	7.95	5.05	2.00	2.49

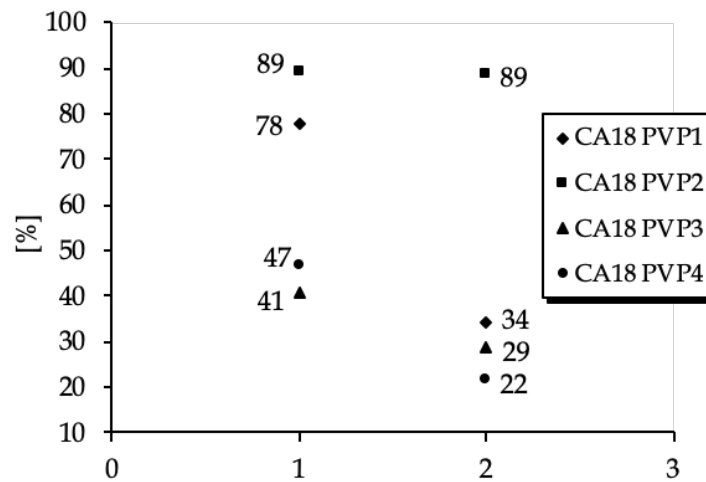


Fig. 4. Phenol rejection of CA18 series membranes after filtration of a phenol solution

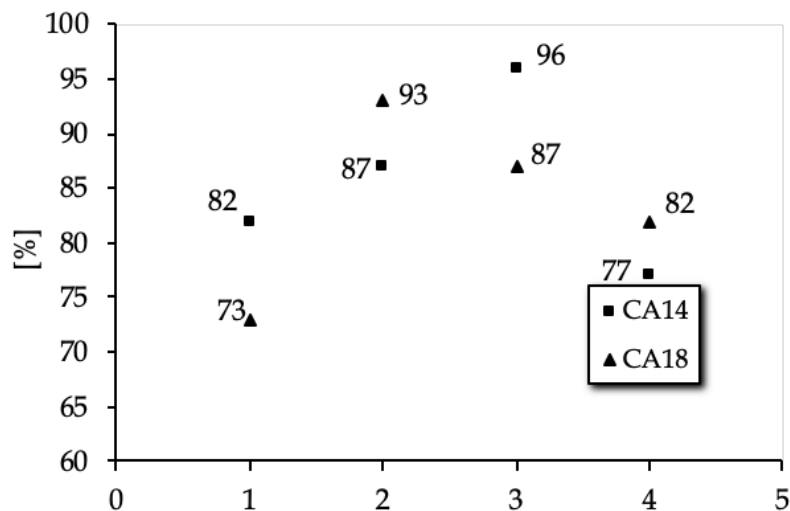


Fig. 5. Flux recovery ratio of CA14 and CA18 series membranes after filtration with 25 mg/L phenol solution

Table 5. Filtration resistance of different membranes for phenol solution (25 mg/L)

Membrane	CA18 PVP1	CA18 PVP2	CA18 PVP3	CA18 PVP4
R_m ($\times 10^{13}$)	15.30	7.51	3.64	3.01
R_p ($\times 10^{13}$)	20.90	8.06	4.15	3.65
R_c ($\times 10^{13}$)	18.00	6.93	3.73	3.38
R_t ($\times 10^{13}$)	54.20	22.50	11.52	10.04

4. Conclusions

Depending on the content of PVP, the membranes obtained have surfaces of different hydrophilicity, however, the addition of PVP does not lead to significant changes in their porosity, equilibrium water content and wetting angle values. Both before and after the filtrations, the oxygen functional groups of acidic character dominate on the membrane surfaces and for most of the CA14 series membranes the number of such groups decreases after the filtration, while for the CA18 series membranes the number of such groups increases after the filtration. The permeability of almost all membranes increases with increasing content of PVP (the exception is sample CA14 PVP1). Moreover, the values of permeability decrease after the filtration as a result of pore blocking. Irrespective of the content of cellulose acetate, all membranes remove phenol more effectively from the solution of the lower concentration. The membranes of CA18 series show better sorption properties. The total resistance of filtration decreases with increasing content of PVP for all membranes except sample CA14 PVP4, and higher values of total resistance show the membranes of CA18 series.

References

- ARASI, M.A., SALEM, A., SALEM, S., 2021. *Production of mesoporous and thermally stable silica powder from low grade kaolin based on eco-friendly template free route via acidification of appropriate zeolite compound for removal of cationic dye from wastewater*. Sustain. Chem. Pharm. 19, 100366.
- BASILE, A., GALLUCCI, F., 2011. *Membranes for Membrane Reactors. Preparation, Optimization and Selection*. John Wiley & sons.
- BAZAN-WOZNIAK, A., PIETRZAK, R., 2020. *Adsorption of organic and inorganic pollutants on activated bio-carbons prepared by chemical activation of residues of supercritical extraction of raw plants*. Chem. Eng. J. 393, 124785.
- BERA, A., BHALANI, D.V., JEWERAKA, S.K., GHOSH, P.K., 2016. *The effect of phenol functionality on the characteristic features and performance of fully aromatic polyester thin film composite nanofiltration membranes*. RSC Adv., 2016,6, 99867-99877.
- DI BELLA, G., DI TRAPANI, D., 2019. *A Brief Review on the Resistance-in-Series Model in Membrane Bioreactors (MBRs)*. Membranes 9(2), 24.
- DING, Y., WU, J., WANG, J., WANG, J., YE, J., LIU, F., 2020. *Superhydrophilic carbonaceous-silver nanofibrous membrane for complex oil/water separation and removal of heavy metal ions, organic dyes and bacteria*. J. Membrane Sci. 614, 118491.
- FANG, J., CHEN, Y., FANG, CH., ZHU, L., 2022. *Regenerable adsorptive membranes prepared by mussel-inspired co-deposition for aqueous dye removal*. Sep. Purif. Technol. 281, 119876.
- GNANASEKARANA, G., ARTHANAREESWARAN, G., MOKA, S., 2021. *A high-flux metal-organic framework membrane (PSF/MIL-100 (Fe)) for the removal of microplastics adsorbing dye contaminants from textile wastewater*. Sep. Purif. Technol. 2021, 119655.
- HERNANDEZ-BARRETO, D., GIRALDO, L., MORENO-PIRAJANA, J.C., 2020. *Dataset on adsorption of phenol onto activated carbons: equilibrium, kinetics and mechanism of adsorption*. Data in Brief 32, 106312.
- HOFMAN, M., PIETRZAK, R., 2011. *Adsorbents obtained from waste tires for NO₂ removal under dry conditions at room temperature*. Chem. Eng. J. 170, 202-208.
- HOOGANTING, M.M., SEWCZYK, A.T., KROLL, S., ARKI, P., BEUTEL, S., REZWAN, K., MAASA, M., 2019. *Proteolytic ceramic capillary membranes for the production of peptides under flow*. Biochem. Eng. J. 145, 89-99.
- HOU, D., FAN, H., JIANG, Q., WANG, J., ZHANG, X. 2014. *Preparation and characterization of PVDF flat-sheet membranes for direct contact membrane distillation*. Sep. Purif. Technol. 135, 211-222.
- JASIEWICZ, K., PIETRZAK, R., 2013. *The influence of pore generating agent on the efficiency of copper and iron ions removal from liquid phase by polyethersulfone membranes*. Chem. Eng. J. 228, 449-454.

- KAMAL, N., AHZI, S., KOCHKODAN, V., 2020. *Polysulfone/halloysite composite membranes with low fouling properties and enhanced compaction resistance*. Appl. Clay. Sci. 199, 105873.
- KRASON, J., PIETRZAK, R., 2018. *Removal of iron and copper ions from the liquid phase by modified polymeric membranes*. J. Polym. Environ. 26, 3237-3242.
- LEON, G., MARTINEZ, G., LEON, L., GUZMAN, M.A., 2016. *Separation of cobalt from nickel using novel ultrasound-prepared supported liquid membranes containing Cyanex 272 as carrier*. Physicochem. Probl. Miner. Process. 52(1) 77-86.
- LI, N.N., FANE, A.G., WINSTON HO, W.S., MASTUURA, T., 2008. *Advanced membrane technology and applications*. New Jersey: Wiley & Sons.
- OCAKOGLU, K., DIZGE, N., COLAK, G., OZAY, Y., BILICI, Z., YALICIN, S.Y., OZDEMIR, S., YATMAZ, H.C., 2021. *Polyethersulfone membranes modified with CZTS nanoparticles for protein and dye separation: Improvement of antifouling and self-cleaning performance*. Colloids Surf. A Physicochem. Eng. Asp. 616, 126430.
- PAN, Y., HANG, Y., ZHAO, X., LIU, G., JIN, W., 2019. *Optimizing separation performance and interfacial adhesion of PDMS/PVDF composite membranes for butanol recovery from aqueous solution*. J. Membrane Sci. 579, 210-218.
- PAUL, B., SARKAR, A., ROY, S., 2021. *Appraising the stress responses in Azolla filiculoides elicited by short-term exposure of phenol*. Plant Stress 2, 100032.
- RUDZANOVA, D., LUPTAKOVA, A., MACINGOVA, E., 2019. *The possibilities of using sulphate-reducing bacteria for phenol degradation*. Physicochem. Probl. Miner. Process. 55(5), 1148-1155.
- SARI, R., CNTERNO, P., DA SILVA, D., DE LIMA, A., OLDONI, T.L.C., THOME, G.R., CARPES, T., 2020. *Extraction of phenolic compounds from tabernaemontana catharinensis leaves and their effect on oxidative stress markers in diabetic rats*. Molecules 25(10), 2391.
- SZCZEPANIK, B., RĘDZIA, N., FRYDEL, L., SŁOMKIEWICZ, P., KOŁBUS, A., STYSZKO, K., DZIOK, T., SAMOJEDEN, B., 2019. *Synthesis and Characterization of Halloysite/Carbon Nanocomposites for Enhanced NSAIDs Adsorption from Water*. Materials 12(22), 3754.
- SOLOMAKOU, N., GOULA, A.M., 2021. *Treatment of olive mill wastewater by adsorption of phenolic compounds*. Rev. Environ. Sci. Biotechnol. 20, 839-863.
- THOMAS, R., GULLIEN-BURRIEZA, E., ARAFAT, H.A., 2014. *Pore structure control of PVDF membranes using a 2-stage coagulation bath phase inversion process for application in membrane distillation (MD)*. J. Membr. Sci. 452, 470-480.
- WU, H., FAN, J., SUN, Y., LIU, R., JIN, J., LI, P., 2021. *Removal of ammonia nitrogen and phenol by pulsed discharge plasma combined with modified zeolite catalyst*. J. Environ. Manage. 299, 113590.
- Zhao, H., WU, L., ZHOU, Z., ZHANG, L., CHEN, H., 2013. *Improving the antifouling property of polysulfone ultrafiltration membrane by incorporation of isocyanate-treated graphene oxide*. Phys. Chem. Chem. Phys. 15, 9084-9092.